



RESEARCH PAPER

UV-induced blue-green and far-red fluorescence along wheat leaves: a potential signature of leaf ageing

S. Meyer¹, A. Cartelat, I. Moya and Z. G. Cerovic

Equipe Photosynthèse et Télédétection, LURE/CNRS, Bât 203, Centre Universitaire Paris-Sud, BP34, F-91898 Orsay Cedex, France

Received 16 September 2002; Accepted 3 October 2002

Abstract

Under UV-excitation, leaves emit red (RF) and far-red (FRF) fluorescence from chlorophyll and blue-green fluorescence (BGF) from hydroxycinnamic acids. In this study, the aim was to develop a fluorescence signature of wheat leaf ageing after the emergence of the lamina. FRF and BGF were examined in the first three leaves of 2-week-old wheat plants. It was investigated how FRF and BGF vary as leaf and tissue aged by spectroscopic measurements, time-resolved BGF analysis and microscopic imaging of the leaf surface. It was found that FRF decreased with leaf and tissue ageing because of an accumulation of UV-absorbers in the epidermis. BGF also decreased, but without changes either in the shape of excitation and emission spectra or in the fluorescence lifetime. So, BGF emanated from the leaf surface, without changes in fluorophore composition during leaf ageing. The shape of the BGF spectrum indicates that ferulic acid bound to the cell wall is the main blue-green fluorophore. The effects of pH and solvents on BGF from intact leaves and ferulic acid in solution were similar, confirming the hydroxycinnamic acid origin of BGF. UV-fluorescence microscopic imaging of the surface of intact leaves showed that different epidermis cell types and sclerenchyma bands emitted BGF. The decreasing gradient of BGF from the base to the apex of the lamina could be related to the decrease in the surface of the fluorescent sclerenchyma bands. The significance of FRF and BGF as potential signatures of wheat lamina growth are discussed.

Key words: Blue-green fluorescence, ferulic acid, fluorescence microscopic imaging, leaf fluorescence, *Triticum aestivum* L.

Introduction

Modern farming has to balance a productionist agriculture with the protection of natural resources, thereby requiring a precise control of crop development in order to determine accurately the amount of inputs needed. UV-induced fluorescence is a potential tool to achieve this control, since it can probe the plant response to stress before visible symptoms occur: it is non-invasive, and it can be remotely and rapidly recorded (Chappelle *et al.*, 1985; Chappelle, 1994; Ounis *et al.*, 2001). Under UV-excitation, green plants emit a red fluorescence (RF, 630–700 nm), a far-red fluorescence (FRF, 700–800 nm), both from chlorophyll, and a blue-green fluorescence (BGF, 400–630 nm) coming mainly from hydroxycinnamic acids (for reviews see Buschmann and Lichtenthaler, 1998; Cerovic *et al.*, 1999). Among the different groups of plants, the monocotyledons, and the Poaceae in particular which comprises the cereals, emitted the brightest BGF because of their large content of ferulic acid bound to cell walls (Harris and Hartley, 1980). This property can potentially be used for probing crop development by UV-induced fluorescence, provided that the origin of the BGF variations is understood.

The information on the anatomical and chemical origins of BGF comes from UV-fluorescence microscopy (Harris and Hartley, 1976; Schnabl *et al.*, 1986; Stober and Lichtenthaler, 1993a; Hutzler *et al.*, 1998), and from *in vivo* fluorescence spectroscopy (Morales *et al.*, 1996; Lichtenthaler and Schweiger, 1998; Cerovic *et al.*, 1999; Johnson *et al.*, 2000). Ferulic acid linked to cell wall polysaccharides by ester bonds was the major fluorophore identified in most plant species showing high BGF. This was revealed by alkali-treatment of leaf transverse sections (Harris and Hartley, 1976; Knogge and Weissenböck, 1986), by the shape of the fluorescence excitation and emission spectra (Morales *et al.*, 1996; Lichtenthaler and

¹ To whom correspondence should be sent: Fax: 33 1 64 46 41 48. E-mail: sylvie.meyer@lure.u-psud.fr

Schweiger, 1998) and by the time-resolved analysis of leaf BGF (Morales *et al.*, 1996). Moreover, it has been shown that the BGF from an intact leaf emanates mainly from the cutinized epidermis both in monocotyledons (Stober and Lichtenthaler, 1993a; Bongli *et al.*, 1994) and in dicotyledons (Bongli *et al.*, 1994; Morales *et al.*, 1998). Therefore, BGF is expected to be dependent on the anatomy of the leaf surface, which varies during leaf development in monocotyledons (Miranda *et al.*, 1981). In addition, the ratio of BGF to RF has been used for remote sensing purposes as a signature of plant health status at different developmental stages under a variable availability of nutrients (Heisel *et al.*, 1996) and under different light conditions affecting leaf development (Stober and Lichtenthaler, 1993a, b). However, in these studies, leaf age has not been taken into account for the interpretation of the ratio. BGF was actually considered as a constant reference to simplify the interpretation of the signature, because the physiological significance of BGF was not fully understood, especially during plant development.

On the other hand, UV-induced RF emanates from mesophyll chloroplasts and depends not only on the chlorophyll content, but also on the flavonoid content of the epidermis vacuoles that screen UV-excitation of the mesophyll (Day *et al.*, 1994; Bilger *et al.*, 1997; Ounis *et al.*, 2001). In monocotyledons, the chlorophyll content increases during leaf development (Boffey *et al.*, 1980). Likewise, the flavonoid content rises (Blume and McLure, 1979; Wiermann, 1981; Knogge and Weissenböck, 1986; Burchard *et al.*, 2000) and, therefore, both the chlorophyll and flavonoid contents can influence the leaf fluorescence signature.

The proportion and the spatial distribution of fluorophores and UV-absorbing compounds can vary independently according to the plant developmental stage. The aim was to understand how it affects leaf UV-induced fluorescence during lamina growth in order to develop fluorescence signatures probing the leaf as tissues age. FRF and BGF were examined in the first three leaves of a wheat plant. BGF variations and origin were interpreted from spectroscopic measurements, time-resolved analysis of BGF and UV-fluorescence microscopy imaging of the leaf surface. Four fluorescence signatures were defined to probe the pattern and the rate of wheat lamina ageing after emergence. The interpretation of the BGF to RF ratio as a probe of leaf ageing is finally examined.

Materials and methods

Plant material

Wheat plants (*Triticum aestivum* cv. Shango) were grown in a growth chamber (Fitotron, Sanyo, Gallenkamp, Leicester, UK), in 0.5 l pots of peat/sand (50:50) with 1 g per pot of a slow release fertilizer (Nutricote 40) and irrigated daily. The temperatures were 24 °C during the day and 18 °C during the night. The irradiance was gradually increased up to 570 $\mu\text{mol photons m}^{-2} \text{s}^{-1}$ and then

decreased to zero and the humidity was decreased to 50% and increased to 70% at the beginning and at the end of the 16 h photoperiod, respectively.

The growth of wheat leaves was monitored by measuring the length of each emerged lamina for 20 d after sowing. This period corresponds to the elongation of the first three leaves.

Chlorophyll dosage

Leaf discs (0.24 cm²) were punched out along the wheat leaf lamina with a cork-borer and immediately immersed in liquid nitrogen. Pigments were extracted by heating the samples for 30 min at 70 °C in 3 ml of methanol for each disc. The extracts were cooled down in darkness. The absorbance of crude extracts was measured on an HP8453 diode-array spectrophotometer (Hewlett-Packard, Les Ulis, France) from 190 to 1100 nm. The chlorophyll concentration was calculated using molar absorptivities and formulae from Lichtenthaler (1987) and corrected for the dilution factor.

Fluorescence measurements

Excitation and emission spectra of intact leaves were acquired between 220–400 and 400–600 nm, respectively, on the FLU3 set-up at the SA4 beam-line of the Super-ACO synchrotron (Orsay, France) (Goulas *et al.*, 1990; Cerovic *et al.*, 1994; Latouche *et al.*, 2000). The high sensitivity of single-photon counting, and high collection efficiency (emission monochromator with an *f/2* aperture ratio) permitted the use of low measuring light levels (less than 0.2 mol m⁻² s⁻¹) that did not induce variable chlorophyll fluorescence. The excitation–detection geometry adapted to front-face measurements (excitation at 50 °C, emission detection at 0 °C) minimized the contribution of scattered light. The use of a double excitation monochromator and of a long-pass filter at emission (KV389, 3 mm Schott, Clichy, France) eliminated completely the second order light problem of diffraction gratings.

Fluorescence spectra of ferulic acid (4-hydroxy-3-methoxycinnamic acid, Sigma, St Louis, MO, USA) were recorded on a spectrofluorimeter (Cary Eclipse, Varian, Les Ulis, France) in a 90° configuration. 1 cm path-length quartz cells (111-QS, Hellma, Paris, France) were used and measurements were made at 20 °C. Ferulic acid was dissolved in a 0.1 M phosphate buffer at variable pH, or in different solvents of spectroscopic grade. The final concentration was 10 μM . Solvents were acidified by adding 6 μl concentrated HCl to 3 ml solvent. Excitation and emission spectra were corrected using Rhodamine B as a photon counter and quinine sulphate as a standard of known emission characteristics, respectively (Miller, 1981). Spectra are, in addition, expressed in quinine sulphate equivalent units (QSEU) (Cerovic *et al.*, 1999). Emission spectra were measured for an excitation wavelength corresponding to the maximum of the absorption spectrum. Excitation spectra were measured for an emission wavelength corresponding to the maximum of the emission spectrum.

The fluorescence lifetime of the adaxial surface of wheat leaves was measured by time-correlated single-photon-counting on the FLU3 set-up, in a front-face configuration, as described in Latouche *et al.* (2000). Decay-histograms were acquired until a total of 2 millions counts were accumulated. Thirty nine nanoseconds were covered by 2048 channels. Fluorescence decays were recorded with an excitation wavelength of 355 nm and an emission wavelength of 450 nm. Deconvolution of the experimental decays into a sum of exponentials was achieved by iterative convolution (Goulas *et al.*, 1990; Cerovic *et al.*, 1994).

BGF and FRF yields from the adaxial surface along the lamina of wheat leaves were measured from 40 plants with a pulse-modulated fluorimeter described in Cerovic *et al.* (1993) and Latouche *et al.* (2000). A high-power xenon flash lamp (L4633, Hamamatsu, Massy, France) was used as a pulsed excitation light source (1 μs duration).

Emission intensities of BGF and FRF were measured with two photodiode-based detectors insensitive to continuous light (Cerovic *et al.*, 1993). The excitation wavelength was defined around 360 nm by the use of three UV transmitting filters: two special absorbing glass filters (DUG11, Schott, Clichy, France) and an interference filter (365HT25, Omega, Brattleboro, USA). A UV-blocking filter (KV408, Schott, Clichy, France) protected the BGF detector, and BGF was further selected using a band-pass filter (450FT690, Corion, Holliston, MA, USA). The FRF detector was protected by two long-pass filters (LG530, Corion, Holliston, MA, USA, and RG 715, Schott, Clichy, France). Excitation light was not actinic, therefore, FRF yield corresponded to the minimal chlorophyll fluorescence (F_0). Fluorescence was monitored from a 5 mm diameter leaf surface. All measurements were made at a controlled temperature of 20 °C, in a front-face configuration.

Fluorescence microscopy imaging

Images of fluorescence were taken using a Zeiss Axiophot epifluorescence microscope (Zeiss, Oberkochen, Germany) equipped with a monochrome cooled CCD camera (Model RTEA/CCD-768K, Princeton Instruments, Inc., USA, NJ) connected to a control unit (Model ST-138, Princeton Instruments). The excitation light was provided by a 50 W mercury vapour lamp (HBO, Zeiss) and the 365 nm mercury line was isolated using a 330WB80 filter (Omega, Brattleboro, USA). It was reflected down on to the sample by a long pass dichroic beam splitter (DCLP400, Omega, Brattleboro, USA) which transmitted the fluorescence to the CCD protected by an LP400 emission filter (Omega). The images of 768×512 pixel size with an 8 bits resolution corresponded to an area of 0.8 and 0.2 mm² with the ×5 and ×10 magnification (Plan-Neofluar quartz objectives, Zeiss), respectively. Experiments were automated using the software Fluograb (Graftek, France) and images were processed using a commercial software Outilab (Concept VI, Graphtek, France).

For determining the relative fluorescence yield, the automatic gain and exposure-time settings were disabled. The gray-scale values were converted into QSEU for each magnification after correction for the absorption of quinine sulphate at 365 nm (mercury line, microscopic measurements) compared to that of the absorption maximum at 347 nm (fluorescence spectra measurements). The fluorescence of quinine sulphate in perchloric acid for a range of concentrations (0–500 nmol quinine sulphate cm⁻²) was imaged on the same microscope in closed round quartz cells (124-QS, Hellma, Paris, France) with an optical path of 0.1 mm. The fluorescence of 1 nmol cm⁻² of quinine sulphate was set to 1000 QSEU as in Cerovic *et al.* (1999). The adaxial surface of intact wheat leaves was always imaged. The relative area of trichomes and epidermal cell walls were determined using routine tools of the software. The relative BGF yield of both trichomes and epidermal cell walls was determined from the relationships between gray-scale and the quinine sulphate fluorescence, in QSEU. This relationship was linear at each magnification.

The relative surfaces of trichomes, guard cells and sclerenchyma bands were determined from photomicrographs of the UV-induced fluorescence of the adaxial leaf surfaces using Kodak Elitechrome 200-ASA film with a LP400 emission filter. In that case, 768×512 pixel images from the scanned film corresponded to 4.8 mm² with ×5 magnification. The UV-induced fluorescence was also monitored from leaves mounted into 10% KOH with a droplet of Tween, or mounted into chloroform. Leaf transverse sections were imaged using a 450WB80 filter (Omega) at emission (in front of the detector).

Statistical analysis was performed with SAS software (SAS Institute Inc., Cary, NC).

Results

Leaf growth

Figure 1 shows the elongation of the lamina after emergence of the first three leaves of wheat plants. The first, second and third leaves were fully expanded 10, 14 and 20 d after sowing, respectively. The growth of monocotyledon leaves is basal. The meristematic and extension zones are enclosed in the sheath and, therefore, the cells of the emerged lamina are completely expanded, but their age increases with distance from the leaf base (Sharman, 1942; Kemp, 1980). As soon as a leaf ceased to grow, a new leaf elongated at a maximal elongation rate of about 4.3 cm d⁻¹ (Fig. 1). The growth of the second and the third leaf reached its maximal rate only 4 d after emergence. This indicates that the apical segment is the slowest segment of the lamina to emerge.

The UV-induced fluorescence was monitored in 46 two-week-old plants, on the first leaf which had ceased to grow for 6 d, the second leaf which was just ending its elongation, and the third leaf which was still growing (Fig. 1). BGF yield was also measured along the second leaf during its elongation from day 10 to day 14 after sowing.

Gradient of UV-induced fluorescence along leaves

The typical fluorescence emission spectrum of a wheat leaf had a blue maximum at 450 nm, and two closely spaced red (686 nm) and far-red maxima (740 nm), (Fig. 2A). The UV-induced fluorescence along intact leaves of a 2-week-old wheat plant was measured in the far-red above 715 nm, to avoid the red fluorescence reabsorption by chlorophyll (Fig. 2B), and in the blue at 450 nm (Fig. 2C). Both FRF

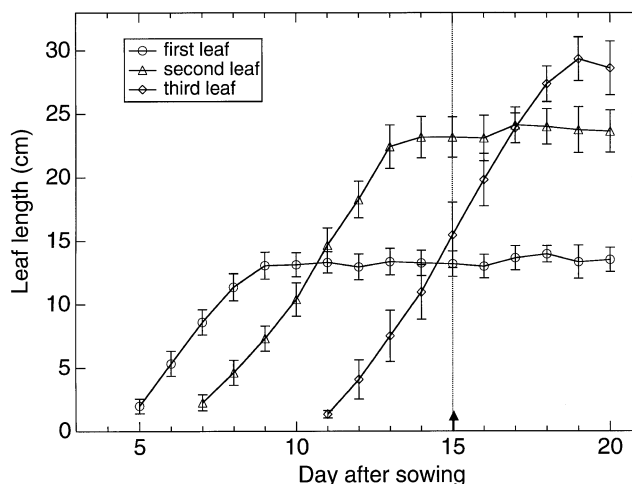


Fig. 1. The dynamics of wheat leaf growth during the first 20 d after sowing. Data are mean \pm SD for 15–102 measurements. The arrow and the dashed line indicate leaves at day 15 used for the experiments depicted in Figs 2 and 4. At this stage of development, the maximal cell age at the tip of the leaf was 11, 9 and 5 d, for the first, the second and the third leaves, respectively.

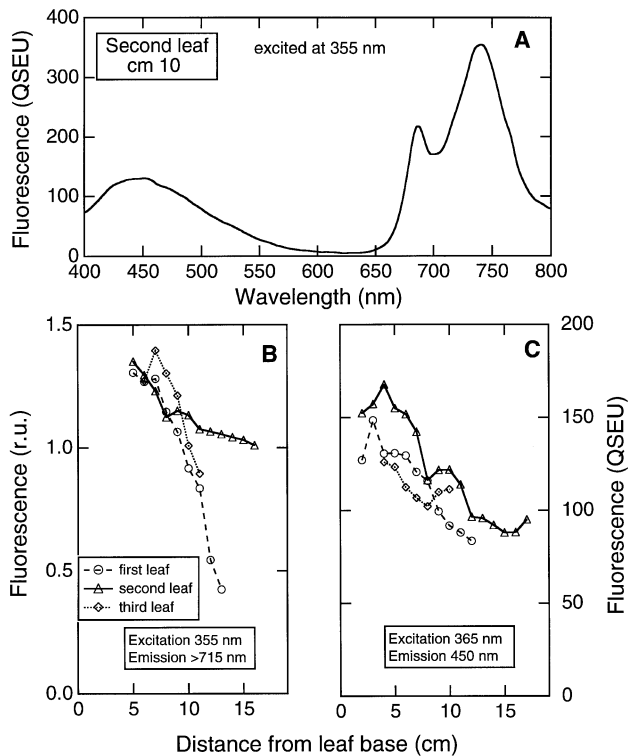


Fig. 2. Fluorescence emission spectrum of a wheat lamina (A) and the variation of FRF (B) and BGF (C) along three leaves of 2-week-old wheat. (A) The emission spectra (excitation at 355 nm) were measured at 10 cm from the base of a second leaf. (B, C) The age of tissues increases with the distance from the leaf base. Data for leaves of a typical plant are shown. Relative BGF yield was expressed in QSEU according to the Materials and methods.

and BGF steadily decreased along all three leaves, showing a negative dependency of the UV-induced fluorescence signature on tissue age, especially in the first leaf (Fig. 2B, C). The decrease in FRF could not be explained by a decrease in chlorophyll content, since the total chlorophyll content increased as cells aged along the lamina (Fig. 3), as usually reported for grasses (Boffey *et al.*, 1980). Total chlorophyll content also increased with tissue age (Fig. 3), whereas chlorophyll fluorescence (FRF) was the lowest in the oldest leaf (cf. Fig. 2B). Therefore, the FRF gradient can only be explained by an accumulation of UV-absorbing compounds in the epidermis, that increasingly screen UV-excitation of the mesophyll. An accumulation of UV-absorbing compounds (flavonoids) in the vacuole of epidermal cells, was already reported during leaf development of cereals (Blume and McLure, 1979; Knogge and Weissenböck, 1986).

The origin of BGF

Excitation and emission spectra of BGF were measured at the base and apex of the three leaves of six 2-week-old plants. The spectra of a typical plant are presented in Fig. 4. The shape of the excitation and emission spectra was

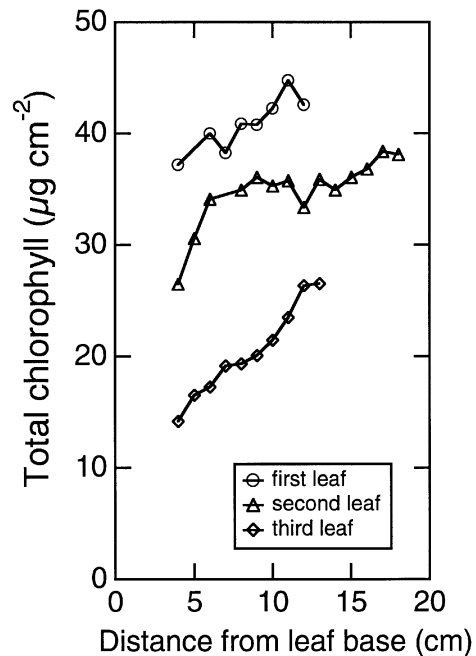


Fig. 3. Total chlorophyll content on a leaf area basis along the three leaves of 2-week-old wheat. The data presented are the means for four leaves. The standard deviation of the mean was between 10% and 13%.

conserved from the base to the apex of each leaf (Fig. 4). Only the emission spectra of the third leaf showed a small shoulder at 530 nm. Whatever the leaf, the BGF excitation efficiency of the oldest segment was smaller than that of younger segments. Since the shape of the excitation spectrum was conserved from the base to the apex of the leaves, the accumulation of UV-absorbing compounds in the epidermis could not be responsible for the weaker BGF of older segments. The fact that the shape of the excitation spectrum did not change along the leaf, nor from the first to the third leaf, indicates that a single set of fluorophores is responsible for a large fraction of BGF. This was confirmed by time-resolved analysis of BGF that yielded similar lifetimes and fractional intensities for the major lifetime components, along the leaf and for all leaf ages (Table 1). The slight, but significant ($P=0.05$), difference in mean lifetime between the base and the apex of the third leaf might be in relation to the green fluorophore revealed by the fluorescence emission spectrum (Fig. 4, small shoulder at 530 nm). Figure 4 and Table 1 reinforce the hypothesis that BGF in wheat leaves originates mostly from the surface, as proposed by Stober and Lichtenhaler (1993a), and by Morales *et al.* (1996) for other species such as sugar beet, since no influence of UV-absorbers present in the underlying cell vacuoles could be detected in BGF excitation spectra.

The excitation maxima at 245 and 335 nm, with a shoulder at 300 nm, and an emission maximum at 460 nm (Fig. 4) indicate that the main blue-green fluorophore is

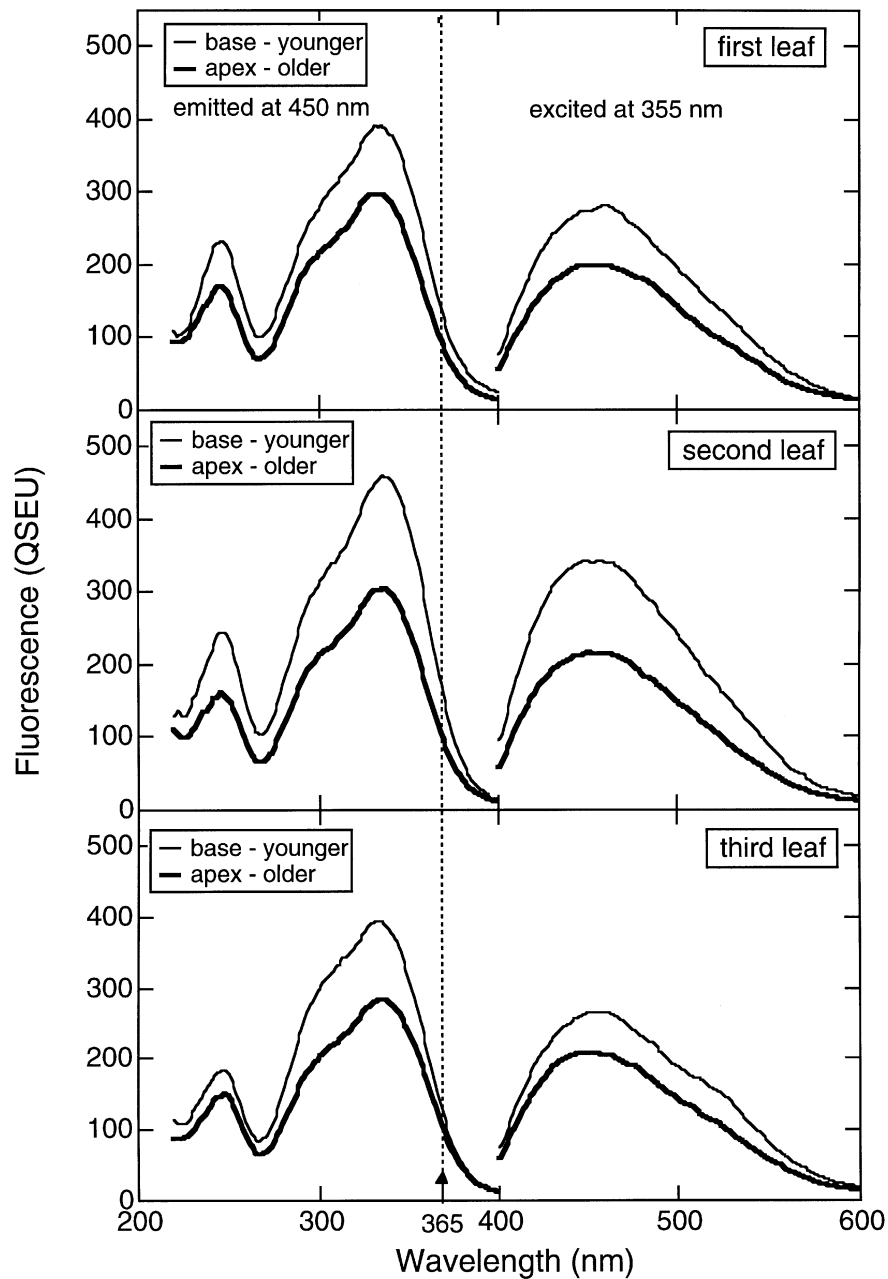


Fig. 4. Excitation (emission at 450 nm) and emission (excitation at 355 nm) fluorescence spectra of three leaves of 2-week-old wheat. Younger base segments (4 cm from the base) and older apex segments (12 cm from the base) from a typical leaf were compared. The dashed line at 365 nm indicates the position of the excitation line of the mercury vapour lamp used in UV-fluorescence microscopy.

probably ferulic acid (Lichtenthaler and Schweiger, 1998). This assignment is further confirmed by the enhancement of epidermal BGF following alkali treatment, and its quenching by immersion into an apolar solvent (Fig. 5). The alkali treatment performed under UV-fluorescence microscopy is a tool to reveal ferulic acid bound to cell walls in the tissues of Poaceae (Harris and Hartley, 1976). pH and solvent effects on the fluorescence spectra of ferulic acid (Fig. 6) explain the microscopic observations (Fig. 5). Ferulic acid is a hydroxycinnamic acid having two

pK_a (4.4 and 9.0, Rasmussen *et al.*, 1995). The non-ionic form (pH 2 and 4) barely fluoresced under UV-A excitation (Fig. 6). A singly-ionized form (pH 6 and 7) was 2-fold more fluorescent, with an excitation maximum at 290–310 nm and an emission maximum around 420 nm. The doubly-ionized form (pH 9 and 10) was the most fluorescent. At pH 10, the maximum excitation and emission were shifted to 345 and 470 nm, respectively, corresponding to the phenolate anion (Jurd, 1957). Under these conditions, the excitation peak of ferulic acid became

Table 1. Mean fluorescence lifetimes (in ns) and fractional intensities of the kinetic components (as a percentage of total fluorescence) at the base and the apex of 2-week-old wheat leaves

The wavelengths of excitation and emission were 355 and 450 nm, respectively. The lifetime of the very fast, fast, medium, and slow kinetic components of the fluorescence decay was 0.11, 0.46, 1.4, and 5.6 ns, respectively. Mean \pm SE are given for four decays. The data were tested for difference between base and apex using Mann and Whitney's *U*-test. *, Significant difference at $P=0.05$.

		Mean lifetime (ns)	Fractional intensity of kinetic component			
			Very fast (%)	Fast (%)	Medium (%)	Slow (%)
First leaf	Base	0.69 \pm 0.032	46 \pm 1.6	31 \pm 1.6	19 \pm 1.6	4 \pm 1.6
	Apex	0.68 \pm 0.013	45 \pm 1.6	32 \pm 1.6	19 \pm 1.6	4 \pm 1.6
Second leaf	Base	0.67 \pm 0.047	42 \pm 1.6	34 \pm 1.6	21 \pm 1.6	3 \pm 1.6
	Apex	0.68 \pm 0.022	42 \pm 3.2	35 \pm 1.6	20 \pm 1.6	4 \pm 1.6
Third leaf	Base	0.59 \pm 0.045*	48 \pm 3.2*	31 \pm 1.6*	19 \pm 1.6	2 \pm 1.6
	Apex	0.66 \pm 0.032*	43 \pm 3.2*	35 \pm 1.6*	20 \pm 1.6	3 \pm 1.6

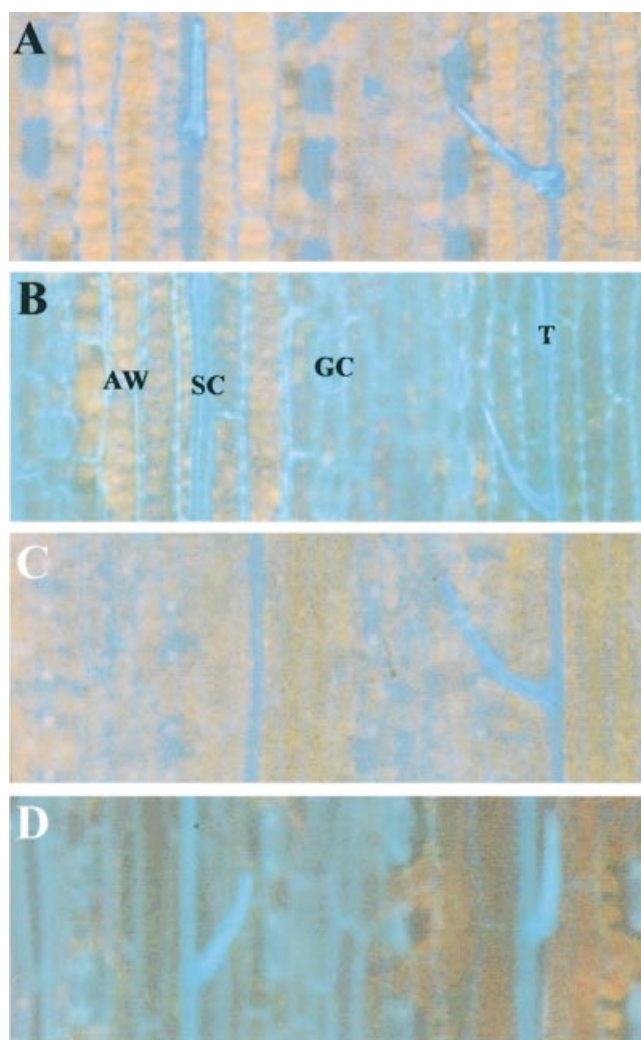


Fig. 5. Effects of pH and solvent on blue-green fluorescence. Colour fluorescence micrographs depict the first leaf adaxial surface from 2-week-old wheat. A control micrograph of an intact leaf was taken (A), then, the leaf was successively treated with 10% KOH for 2 min (B), chloroform for 40 s (C), and 10% KOH for 2 min (D). Images correspond to 0.3 mm² leaf area. The exposure time was 10 s for each micrograph. AW; anticlinal wall of epidermal cell, SC; sclerenchyma band, GC; guard cell, T; trichome.

closer to the excitation line of the mercury vapour lamp used for microscopy (365 nm). Consequently, the alkali-treatment of the leaf surface enhanced BGF (Fig. 5) because the phenolate ion of ferulic acid was more efficiently excited.

The solvent polarity also affected the fluorescence spectra of ferulic acid (Fig. 6B). With the decreasing polarity of the solvent, the excitation and emission of BGF from the ferulic acid solution and the Stokes shift decreased (Fig. 6B). In an apolar solvent (chloroform), BGF of ferulic acid was quenched by 80% with respect to the situation in a polar solvent (water). In chloroform, the excitation of ferulic acid was very weak at 365 nm (Fig. 6B), which explains the decrease of leaf BGF (Fig. 5C). However, a subsequent alkali-treatment (Fig. 5D) did not fully reverse this decrease, suggesting that chloroform removed the waxes of the cuticle where some blue-green fluorophores might also have been embedded (Karabourniotis *et al.*, 1992). It is known that the cuticle may contain esters of ferulic acid and other hydroxycinnamic acids (Kolattukudy, 1980).

Relationship between BGF and the anatomy of the leaf surface

The adaxial epidermis of wheat leaves is formed of long cells with non-sinuuous walls, some solitary short cells over the vein, stomata with subsidiary cells, short hairs with a swollen base, and sclerenchyma bands. As seen in Fig. 5, the wall of each epidermal cell type, trichome protoplast and lignified sclerenchyma bands emitted BGF.

The leaf surface is a complex mosaic of several fluorescent cell types. Hence, both the proportion of the different cell types and cell BGF intensity will determine the BGF measured at the leaf level (as in Fig. 2 on a 5 mm² leaf area). It is, therefore, important to know the relative surface and BGF yield of the different cell types. Table 2 summarizes the results of the microscopic analysis of the base (young) and the apex (old) of the first three leaves of 2-week-old wheat plants. The relative surface of the

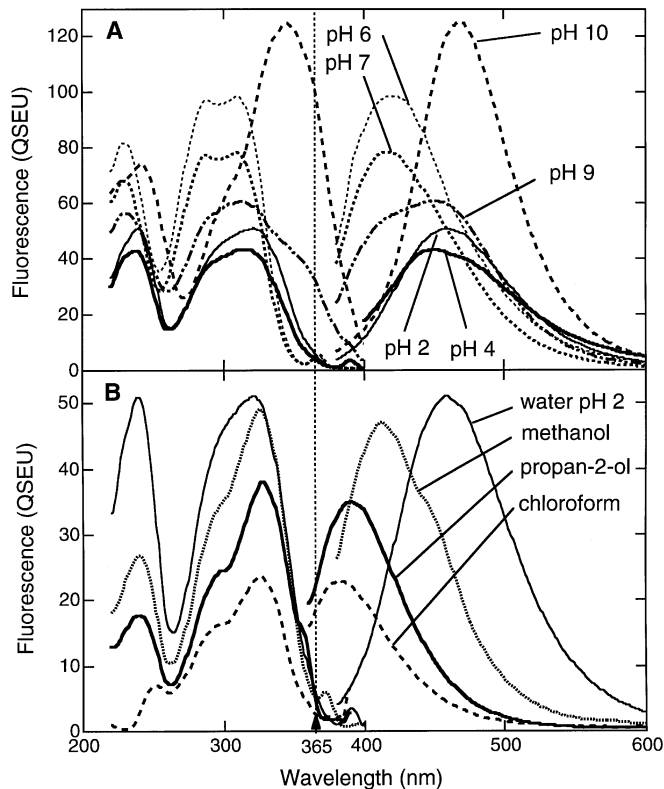


Fig. 6. Fluorescence excitation and emission spectra of ferulic acid (10 μ M) in solution. Excitation spectra were recorded at the emission maximum in the blue. Emission spectra were recorded at the absorption maximum in the UV-A. (A) Ferulic acid in phosphate buffer at different pH. Ferulic acid was in non-ionic, singly and doubly-ionized form at pH 2–4, 6–7 and 9–10, respectively. (B) Ferulic acid in different acidified solvents, whose polarity decreased starting from water ending with chloroform. The dashed line at 365 nm indicates the excitation line of the mercury vapour lamp used in UV-fluorescence microscopy. The small sharp peak in excitation spectra seen above 350 nm is due to the Raman scattering of the solvent.

anticlinal cell wall and the trichomes (including wall and protoplast) significantly increased along the leaves, but their relative fluorescence yield decreased. The two effects compensate each other, therefore, variation of these particular structures along the leaf cannot explain the BGF gradient shown in Fig. 2. On the other hand, the relative surface of the sclerenchyma band significantly decreased from the base to the apex of the second and third leaves. The significant increase in the sclerenchyma BGF yield of the second leaf did not compensate for it. This suggests that the gradient of BGF along the leaf was related to the reduction of the surface of fluorescent sclerenchyma bands.

Further experiments were then performed to determine if a relationship between BGF and the relative surface of the sclerenchyma bands persisted during the course of leaf growth. BGF and anatomical measurements were performed on consecutive days after sowing along the second leaf, in which the developmental gradient along the lamina was maximal 14 d after sowing. Figure 7 summarizes the BGF and anatomical variations along the second leaf of different ages from ten to fourteen days after sowing. To compare leaves at different stages of elongation, the results were presented by making the leaf tips coincide in order to take into account the basal growth of the lamina. The gradients of BGF or the anatomical traits of each leaf age superimposed to give a unique relationship. This shows that, BGF and anatomical traits measured in these experiments were dependent on the ontogenetic pattern of the leaf, which was determined before the lamina segments emerged. An obvious parallelism between BGF gradients and the sclerenchyma band's relative surface along the leaves is prominent. At the base, on the youngest segment, sclerenchyma covered 10% of the area, whereas at the apex, the oldest segment, it covered about 5%. Concomitantly, BGF decreased by 50% from the base to

Table 2. Relative leaf surface (%) and BGF yield (QSEU) of the anticlinal cell wall, trichome and sclerenchyma bands from adaxial epidermis of the first three leaves of 2-week-old wheat

Data are mean \pm SE. The number of images is indicated in brackets. Images from the base and the apex were taken from 0–30% and from 70–100% of the leaf length, respectively. For anticlinal cell walls or trichomes analysis, each relative surface and BGF was determined from leaf areas of 0.8 mm². The analysis of sclerenchyma band, the relative surface and BGF were determined from leaf areas of 4.8 and 0.8 mm², respectively. SM: a single measurement is available with a value of 1500 QSEU. The data were tested for difference between base and apex using Mann and Whitney's *U*-test. **, significant difference at $P=0.01$; *, $P=0.05$; NS, not significant.

		Anticlinal cell wall		Trichome		Sclerenchyma bands	
		Surface (%)	BGF (QSEU)	Surface (%)	BGF (QSEU)	Surface (%)	BGF (QSEU)
First leaf	Base	6.0 \pm 0.45*(15)	4643 \pm 326*(15)	1.4 \pm 0.36*(18)	4359 \pm 403**(18)	6.5 \pm 9.42 NS(3)	3409 \pm 525 NS(14)
	Apex	6.9 \pm 0.49(11)	3541 \pm 864(11)	1.8 \pm 0.32(17)	3593 \pm 555(17)	5.7 \pm 1.20(7)	2955 \pm 1335(5)
Second leaf	Base	8.1 \pm 0.90**(9)	4356 \pm 466**(9)	2.9 \pm 1.33*(10)	4540 \pm 545 NS(10)	10.1 \pm 4.47*(5)	2655 \pm 215**(8)
	Apex	10.7 \pm 1.21(8)	3495 \pm 608(8)	4.4 \pm 0.97(8)	3819 \pm 435(8)	3.9 \pm 1.70(6)	3059 \pm 51(2)
Third leaf	Base	7.0 \pm 0.61*(13)	4261 \pm 442**(13)	1.8 \pm 0.62**(12)	3988 \pm 357**(12)	8.5 \pm 2.03**(5)	3417 \pm 504(8)
	Apex	7.9 \pm 0.56(11)	2281 \pm 287(11)	5.2 \pm 1.21(16)	2350 \pm 300(16)	4.5 \pm 1.76(7)	SM

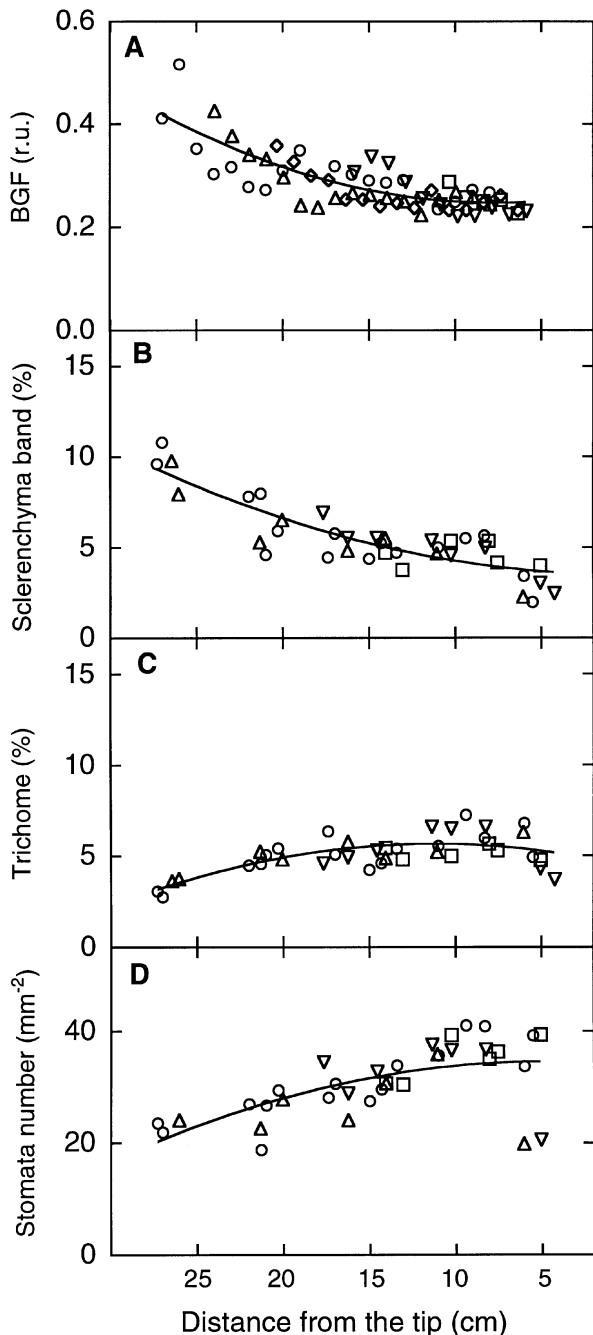


Fig. 7. Gradients of BGF and anatomy along the second wheat leaf during its elongation. Unlike Figs 3 and 4, where the leaf zero distance corresponds to the ligule, the basal growth has been taken into account. This was achieved by making the tips, the oldest segments of the leaves, coincide. Typical leaves are shown. BGF (A) and relative areas of sclerenchyma bands (B), trichome (C), and the stomata number mm^{-2} (D) were measured along the adaxial face of the leaf, 10 (open squares), 11 (open inverted triangles), 12 (open circles), and 14 (open triangles) d after sowing. The 5% relative surface of trichomes corresponded to about 16 trichomes mm^{-2} . Fit was according to a second order polynomial with r^2 equal to 0.80, 0.86, 0.70, and 0.63 from (A) through (D), respectively.

the apex. By contrast, the BGF gradient along the leaf was not related to the variation of trichome relative surface or stomata number per mm^2 , which both increased towards the tip of a growing leaf (Fig. 7). At the tip of the leaf, sclerenchyma band and trichome relative surface and stomata number per mm^2 were particularly low. This was the oldest segment of the lamina, which had emerged when leaf development was the slowest (Fig. 1).

Figure 8 shows images of the UV-induced fluorescence of different segments along a young and a mature leaf. BGF and FRF emanated from the epidermis and the underlying mesophyll, respectively. Images illustrate that, as the leaf elongated, the sclerenchyma bands of the emerged segment became wider but fewer. In Fig. 8, the anatomy of the different segments of a young (10-d-old) and a mature (14-d-old) leaf are compared side by side by making the leaf tips coincide. The segment at 3 cm from the base of the young leaf will be at a distance approximately 15 cm from the base 4 d later (mature leaf), without a noticeable change in leaf surface anatomy. By contrast, the surface anatomy of the segment 3 cm from the base in the young leaf and in the mature leaf were quite different, illustrating the ontogenetic pattern of the lamina. Figure 8 shows that the BGF is a signature of this ontogenetic pattern because it depends on the development of the sclerenchyma bands (cf. Fig. 7).

A transverse section of a leaf (Fig. 8, inset) shows that the sclerenchyma bands are constituted of narrow fibres with thick walls that fluoresce brightly at 450 nm. The walls are lignified because they gave a positive test with phloroglucinol-HCl (data not shown). Sclerenchyma fibres are dead cells, therefore only their wall absorbed UV. The BGF from the sclerenchyma bands excited by illuminating the surface of an intact leaf (Fig. 8) may be emitted from several layers of fibres (Fig. 8, inset). Sclerenchyma cells were surrounded by long epidermal cells, whose anticlinal and periclinal walls also fluoresced at 450 nm. However, the vacuolar content of these cells might screen the UV-excitation of the underlying periclinal cell wall when measurements were performed on the intact leaf.

A double fluorescence signature of the leaf elongation

Considering the emerged lamina as a whole at different days after sowing, it appears that BGF increased by 36% as the leaf aged (Table 3). This again was related to the broadening of sclerenchyma bands at the base of the lamina, as the leaf grew. Conversely, chlorophyll fluorescence (FRF) decreased by 37% as the leaf aged, which could be explained by the accumulation of UV-screening compounds with time. Therefore, Table 3 shows that both fluorescence signatures can be used as signatures of leaf elongation. Since the relative variations of BGF and FRF were opposite, the ratio between BGF and FRF varied greatly during leaf elongation. The ratio was twice as important in mature than in young leaves. Hence, the BGF/

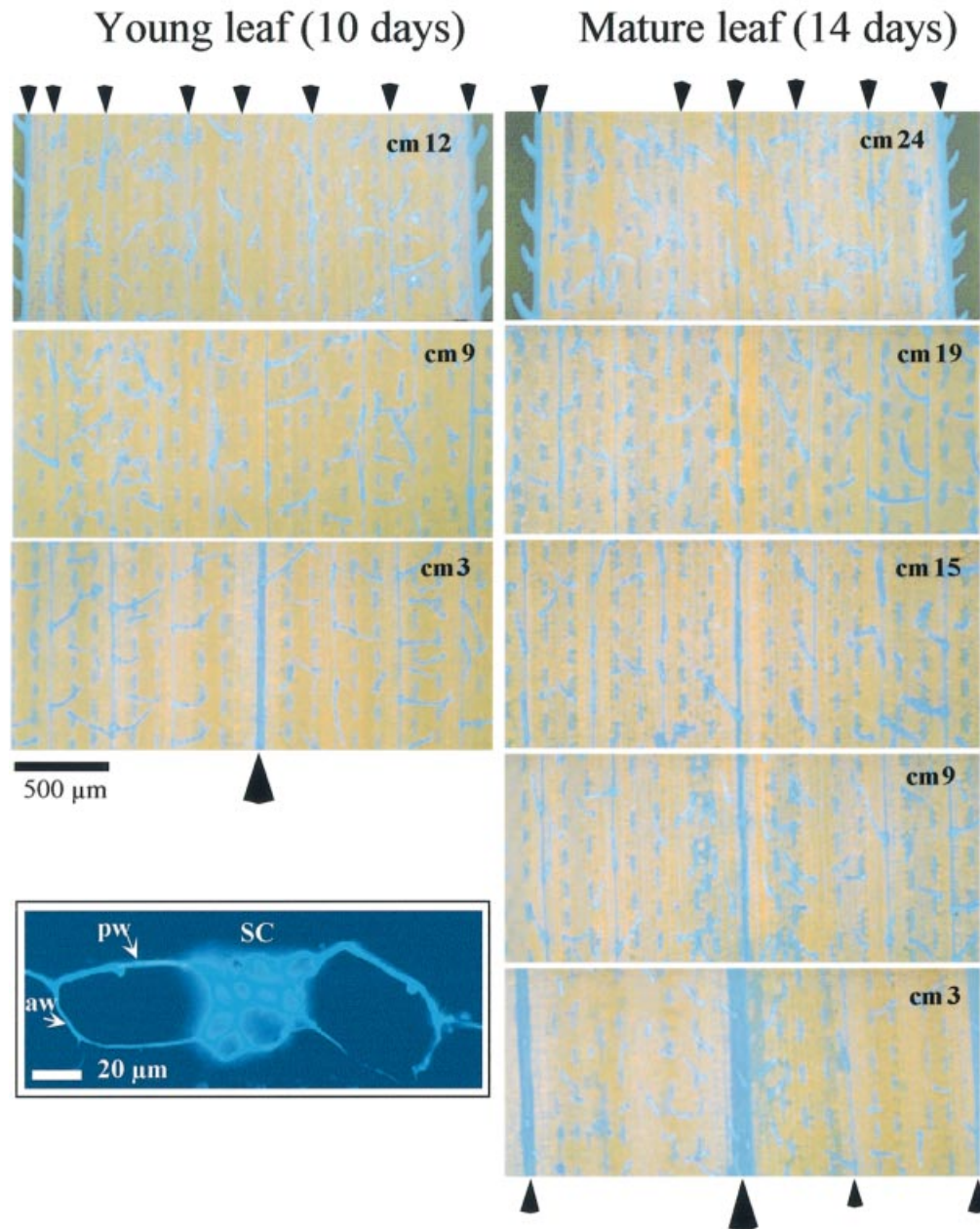


Fig. 8. Colour fluorescence images along the adaxial face of a second wheat leaf at different stages of elongation. A young leaf and a mature leaf were imaged 10 d and 14 d after sowing, respectively, using an LP400 emission filter. The distance from the leaf base of each imaged segment is indicated. The arrows indicate the position of the sclerenchyma bands. Ten days after sowing, the segments at 3, 9 and 12 cm from the base are 0.8, 2.4 and 3.2-d-old. Fourteen days after sowing, the segments at 3, 9, 15, 19, and 24 cm from the base are 1.8, 3.4, 5.0, 6.1, and 7.5-d-old, respectively. The inset shows a transverse section of adaxial epidermis imaged with a 450WB80 emission filter. SC; sclerenchyma band, aw; anticlinal wall, pw; periclinal wall.

FRF ratio was a very sensitive signature of leaf growth, but its interpretation required an independent monitoring of BGF and FRF, as shown in Table 3.

Discussion

In this study an analysis was undertaken of the variation of UV-induced BGF measured from the surface of intact wheat leaves according to the age of the cell or

of the segment along the lamina, and during the ageing of the leaf from emergence to maturity. The spectral characteristics of BGF along the leaves of different ages were shown to be that of a hydroxycinnamic acid, most probably ferulic acid. Excitation and emission spectra were not deformed by reabsorption or screening effects, indicating that BGF emanated primarily from the surface of the lamina, in agreement with Stober and Lichtenthaler (1993a).

Table 3. Mean BGF and FRF per unit surface of the total leaf surfaces of a second leaf during its growth

Fluorescence was excited at 355 nm and measured at 450 nm and above 715 nm for BGF and FRF, respectively. BGF/FRF is indicated. Mean \pm SE are given for four leaves at each day after sowing. Results are also expressed as a percentage of the value from the youngest developmental stage (day 10). The data (r.u.) were tested for difference with respect to the leaf at 10 d after sowing, using Mann and Whitney's *U*-test. *, significant difference at $P=0.05$; NS, not significant.

Days after sowing	BGF		FRF		BGF/FRF	
	(r.u.)	(%)	(r.u.)	(%)		(%)
10	0.25 \pm 0.006	100	1.69 \pm 0.318	100	0.15	100
11	0.26 \pm 0.022 NS	104	1.55 \pm 0.086 NS	92	0.17*	113
12	0.26 \pm 0.013 NS	104	1.53 \pm 0.264 NS	91	0.27*	180
13	0.29 \pm 0.025*	116	1.36 \pm 0.108 NS	80	0.21*	140
14	0.30 \pm 0.095*	120	1.46 \pm 0.073 NS	86	0.21*	140
15	0.34 \pm 0.013*	136	1.06 \pm 0.121*	63	0.32*	213

By imaging the leaf adaxial surface, it was shown that BGF emanated from the wall of diverse cell types, whose relative surface, spatial distribution and relative fluorescence yield could control BGF emission. At the cellular level, there was a general decrease in the intrinsic BGF yield of anticlinal cell walls and the trichome from the base to the apex of the lamina, which might indicate that the cell wall differentiation affected the fluorescence of ferulic acid. This might be an indication of changes in surface content of ferulic acid. Phenyl ammonia lyase (PAL) activity was reported to be larger at the base than at the apex of the lamina of *Avena* (Wiermann, 1981), suggesting a larger hydroxycinnamic acid content at the leaf base. Ferulic acid is known to contribute to wall rigidification (Fry, 1986). A decrease in extractable ferulic acid on a leaf area basis, resulting from a decrease in wall-bound ferulic acid esters concomitant with an increase in ferulic acid ester-ether bridges and with cell wall lignification, has already been reported in leaves of developing wheat seedlings (Strack *et al.*, 1987; Lam *et al.*, 1996). However, the BGF of lignin and of the different wall-bound forms of ferulic acid and diferulic acid remains to be studied.

A decrease in apoplastic pH or/and polarity could also be responsible for the decrease in ferulic acid fluorescence from cell walls as the cell aged along the lamina. Grignon and Sentenac (1991) indicated that leaf apoplastic pH lies between 5 and 6.5 and Hill *et al.* (2002) reported that old leaves of a wild monocot species have a lower apoplastic pH than young leaves (pH 6.2 and 5.5 for young and old leaves, respectively). At these pH, soluble ferulic acid barely fluoresced under UV-excitation at 365 nm because the phenol group is not ionized (Jurd, 1957), suggesting that other cellular parameters have to be taken into account to interpret the epidermal BGF *in vivo*. Still, for ferulic acid esterified to cell walls, the carboxyl group can not be ionized because it is engaged in the ester bond. Therefore, the emission spectrum of bound ferulic acid should correspond to the one measured at pH 2 *in vitro* for free ferulic acid (below the first pK_a) (Fig. 6). This would explain the maximum leaf BGF emission at 460 nm *in vivo*.

On the other hand, a decrease in polarity quenched soluble ferulic acid fluorescence yield and induced a bathochromic shift of the excitation maximum *in vitro*. This is a conventional effect of a lipophilic solvent on fluorochrome (for a review see Valeur, 1993). It might occur as cuticles differentiate on the periclinal wall along the leaf, especially for the first leaf, in which the decrease in BGF was the least related to a reduction in relative surface of sclerenchyma bands (Fig. 2; Table 2). According to Sharman (1942), Miranda *et al.* (1981) and Riederer and Schönherr (1988), cuticle thickness increases along the leaf of monocotyledons and the polarity of the cuticle decreased (Schmidt and Schönherr, 1982). The consequence of the cuticular differentiation on leaf BGF awaits further studies. Considering the sensitivity of ferulic acid in solution to pH and polarity, the four lifetime components of leaf fluorescence decay could correspond to different cellular environments of ferulic acid. Spectral time-resolved investigations should be performed to analyse ferulic acid BGF *in vivo* and *in vitro* in order to estimate if it could be a signature of the leaf apoplastic properties, such as pH, polarity or viscosity.

At the leaf level, the epidermal cell differentiation during lamina elongation did not affect BGF signature. This was explained by a compensatory effect between the increase in the cell-wall relative surface and the decrease in relative cell-wall BGF yield. BGF decreased along the leaf mainly because of a reduction in the relative surface of fluorescing sclerenchyma, even though this tissue corresponds to only 5 to 10% of the leaf area.

The conserved shape of excitation and emission spectra and the conserved mean fluorescence lifetime and fractional intensity of kinetic components indicated that, at this scale of measurement, no concomitant change in composition of the fluorophore occurred. The 4–5 mm² of lamina used for measurements comprised veins and intercostal areas. It should be representative of the general structure of the leaf surface (the lamina width was about 5 mm). Since BGF varied according to the development of the sclerenchyma bands, which gradually provided an

increased support function as the lamina elongated, BGF could be interpreted as a signature of the ontogenetic pattern of the lamina.

The decrease in FRF with cell age along the lamina and as the lamina elongated, which was not related to the increase in the chlorophyll content, was explained by an accumulation of UV-absorbing compounds in the epidermis. It is known that flavonoids accumulate during the growth of Poaceae lamina, as in *Avena* (Wiermann, 1981). Flavonoids mainly accumulated in the vacuole of the epidermis (Schnabl *et al.*, 1986) and screened UV-excitation of the mesophyll (Day *et al.*, 1994). In these experiments, this screening effect obviously increased with cell and leaf age, because it fully overrides the rise in chlorophyll content during leaf development. In wheat leaves, iso-orientine and tricine are the main flavonoids (Estiarte *et al.*, 1999). Since flavonoids are increasingly accumulated with the duration of exposure of the plant to light (McClure and Wilson, 1970), the decrease in FRF during leaf development can be a measure of the time elapsed since a segment or a whole leaf has emerged. Therefore, FRF could also be considered as a physiological clock of leaf development.

In this study, it has been shown that the FRF and BGF emissions depend on two causes: the accumulation of UV-absorber in the epidermis and the development of sclerenchyma fibres, respectively. However, because of their independent variation, four signatures can be defined to probe wheat lamina development after emergence (Fig. 9): (i) a concomitant decrease of BGF and FRF along the lamina probes the process of cell ageing (Fig. 2, Fig. 9 arrow 1), (ii) an unchanged BGF with time, while FRF decreases, is a signature of the time which elapsed since the emergence of the segment (Fig. 9 arrow 2), (iii) an increasing BGF with time, while FRF remains constant, signs the ontogenetic pattern of the leaf (Fig. 9 arrow 3), (iv) a concomitant increase in BGF and decrease in FRF with time reflects the process of whole leaf ageing (Fig. 9, arrow 4). The signature of the ontogenetic (arrow 3) pattern can be a potential identity card of the cereal species, since they differ in the anatomy of their leaf surface (Metcalfe, 1960). Further, this signature, with the two others probing the rate of lamina elongation (arrows 1 and 2), potentially allow a nutrient deficiency to be detected, because the elongation rate and the sclerenchyma development of cereal leaves depend on the nutrient availability in the soil (Van Arendonk *et al.*, 1997). These fluorescence signatures are presently being applied to studies in the field on a wheat crop subject to differing nitrogen supply (A Cartelat, S Meyer, ZG Cerovic, unpublished results).

Knowing the significance of BGF and FRF signatures in wheat, the BGF/FRF ratio becomes of particular interest to probe the leaf growth. The BGF/FRF ratio is highly sensitive to leaf age, because of the opposite behaviour of

BGF and FRF. This explains the large change of this ratio seen in cereals (Chappelle *et al.*, 1985; Stober and Lichtenthaler, 1993a, b; Heisel *et al.*, 1996). Moreover, this ratio is inherently insensitive to excitation light inhomogeneity and it is potentially independent of measuring distance. This allows its use as a signature for remote sensing of crops (cf. Heisel *et al.*, 1996) by probing leaf growth.

Acknowledgements

We thank S Yakovlev (Evolution et Systématique, Université Paris Sud, France) for the use of the epifluorescence microscopy imaging device, M Laurent (Service d'imagerie, Université Paris Sud, France) for the use of an epifluorescence microscope, Y Le Breton (ITCF, France) for providing the seeds, and R Guérin from the Fertel Company for the gift of Nutricote. We thank JM Ducruet (EPT, LURE, France) and Henrik Davi (Ecologie Végétale, Université Paris Sud, France) for helpful comments on the manuscript. We acknowledge the support of the CNRS through the GDR 1536 'FLUOVEG'.

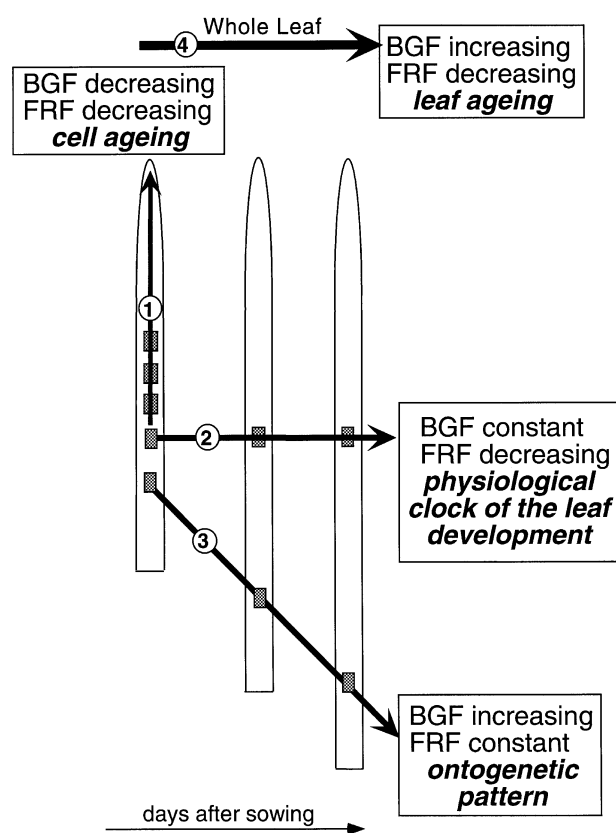


Fig. 9. Potential UV-induced fluorescence signatures of wheat leaf development. A lamina is represented at different stages of elongation. Three situations are depicted: segments along the leaf have different ontogeny and increasing age (1); the segment present at a constant distance from the tip is only ageing (2); emerging segments at a constant distance from the base have the same age but have a different ontogeny (3). The UV-induced fluorescence signatures and their interpretation are indicated in boxes. Whole leaf ageing is indicated by the arrow No. 4.

References

- Bilger W, Veit M, Schreiber L, Schreiber U.** 1997. Measurement of leaf epidermal transmittance of UV radiation by chlorophyll fluorescence *Physiologia Plantarum* **101**, 754–763.
- Blume D, McLure J.** 1979. Developmental changes in flavonoids and enzyme activities of primary leaves from field-grown barley. *Zeitschrift für Pflanzenphysiologie* **95**, 121–128.
- Boffey SA, Selden G, Leech RM.** 1980. Influence of cell age on chlorophyll formation in light-grown and etiolated wheat seedlings. *Plant Physiology* **65**, 680–684.
- Bongi G, Palliotti A, Rocchi P, Moya I, Goulas Y.** 1994. Blue-green fluorescence excited by UV laser on leaves of different species originates from cutin and is sensitive to leaf temperature. *Plant, Cell and Environment* **17**, 777–780.
- Burchard P, Bilger W, Weissenböck G.** 2000. Contribution of hydroxycinnamates and flavonoids to epidermal shielding of UV-A and UV-B radiation in developing rye primary leaves as assessed by ultraviolet-induced chlorophyll fluorescence measurements. *Plant, Cell and Environment* **23**, 1373–1380.
- Buschmann C, Lichtenthaler HK.** 1998. Principles and characteristics of multi-colour fluorescence imaging of plants *Journal of Plant Physiology* **152**, 297–314.
- Cerovic ZG, Bergher M, Goulas Y, Tosti S, Moya I.** 1993. Simultaneous measurement of changes in red and blue fluorescence in illuminated isolated chloroplasts and leaf pieces: the contribution of NADPH to the blue fluorescence signal. *Photosynthesis Research* **36**, 193–204.
- Cerovic ZG, Morales F, Moya I.** 1994. Time-resolved spectral studies of blue-green fluorescence of leaves, mesophyll and chloroplasts of sugar beet (*Beta vulgaris* L.). *Biochimica et Biophysica Acta* **1188**, 58–68.
- Cerovic ZG, Samson G, Morales F, Tremblay N, Moya I.** 1999. Ultraviolet-induced fluorescence for plant monitoring: present state and prospects. *Agronomie: Agriculture and Environment* **19**, 543–578.
- Chappelle EW.** 1994. Special issue of Remote Sensing of Environment. In: Chappelle EW, ed. *Remote sensing of environment*. New York: Elsevier.
- Chappelle EW, Wood FM, Newcomb WW, McMurtrey JE.** 1985. Laser-induced fluorescence of green plants. 3. LIF spectral signatures of five major plant types. *Applied Optics* **24**, 74–80.
- Day TA, Howells BW, Rice WJ.** 1994. Ultraviolet absorption and epidermal-transmittance spectra in foliage. *Physiologia Plantarum* **92**, 207–218.
- Estiarte M, Penuelas J, Kimball BA, Hendrix DL, Pinter PJ, Wall GW, LaMorte RL, Hunsaker DJ.** 1999. Free-air CO₂ enrichment of wheat: leaf flavonoid concentration throughout the growth cycle. *Physiologia Plantarum* **105**, 423–433.
- Fry SC.** 1986. Cross-linking of matrix polymers in the growing cell walls of angiosperms. *Annual Review of Plant Physiology and Plant Molecular Biology* **37**, 165–186.
- Goulas Y, Moya I, Schmuck G.** 1990. Time-resolved spectroscopy of the blue fluorescence of spinach leaves. *Photosynthesis Research* **25**, 299–307.
- Grignon C, Sentenac H.** 1991. pH and ionic conditions in the apoplast. *Annual Review of Plant Physiology and Plant Molecular Biology* **42**, 103–128.
- Harris PJ, Hartley RD.** 1976. Detection of bound ferulic acid in the cell walls of the Gramineae by ultraviolet fluorescence microscopy. *Nature* **259**, 508–510.
- Harris PJ, Hartley RD.** 1980. Phenolic constituents of the cell walls of monocotyledons. *Biochemical Systematics and Ecology* **8**, 153–160.
- Heisel F, Sowinska M, Miehe JA, Lang M, Lichtenthaler HK.** 1996. Detection of nutrient deficiencies of maize by laser induced fluorescence imaging. *Journal of Plant Physiology* **148**, 622–631.
- Hill PW, Raven JA, Sutton MA.** 2002. Leaf age-related differences in apoplastic NH₄⁺ concentration, pH and the NH₃ compensation point for a wild perennial. *Journal of Experimental Botany* **53**, 277–286.
- Hutzler P, Fischbach R, Heller W, Jungblut TP, Reuber S, Schmitz R, Veit M, Weissenböck G, Schnitzler J-P.** 1998. Tissue localization of phenolic compounds in plants by confocal laser scanning microscopy. *Journal of Experimental Botany* **49**, 953–965.
- Johnson GA, Mantha SV, Day TA.** 2000. A spectrofluorometric survey of UV-induced blue-green fluorescence in foliage of 35 species. *Journal of Plant Physiology* **156**, 242–252.
- Jurd L.** 1957. The detection of aromatic acids in plant extracts by ultraviolet absorption spectra of their ions. *Archives of Biochemistry and Biophysics* **66**, 284–288.
- Karabourniotis G, Padopoulos K, Papamarkou M, Manetas Y.** 1992. Ultraviolet-B radiation absorbing capacity of leaf hairs. *Physiologia Plantarum* **86**, 414–418.
- Kemp DR.** 1980. The location and size of the extension zone of emerging wheat leaves. *New Phytologist* **84**, 729–737.
- Knogge W, Weissenböck G.** 1986. Tissue-distribution of secondary phenolic biosynthesis in developing primary leaves of *Avena sativa* L. *Planta* **167**, 196–205.
- Kolattukudy PE.** 1980. Biopolyester membranes of plants: cutin and suberin. *Science* **208**, 990–1000.
- Lam TBT, Iiyama K, Stone BA.** 1996. Caffeic acid: *o*-methyltransferases and biosynthesis of ferulic acid in primary cell walls of wheat seedlings. *Phytochemistry* **41**, 1507–1510.
- Latouche G, Cerovic ZG, Montagnini F, Moya I.** 2000. Light-induced changes of NADPH fluorescence in isolated chloroplasts: a spectral and fluorescence lifetime study. *Biochimica et Biophysica Acta* **1460**, 311–329.
- Lichtenthaler H.** 1987. Chlorophylls and carotenoids: pigments of photosynthetic biomembranes *Methods in Enzymology* **148**, 350–382.
- Lichtenthaler HK, Schweiger J.** 1998. Cell wall bound ferulic acid, the major substance of the blue-green fluorescence emission of plants. *Journal of Plant Physiology* **152**, 272–282.
- McClure JW, Wilson KG.** 1970. Photocontrol of C-glycosylflavones in barley seedlings. *Phytochemistry* **9**, 763–773.
- Metcalfe C.** 1960. *Anatomy of monocotyledons*. Oxford: Clarendon Press.
- Miller J.** 1981. Correction of excitation and emission spectra. In: Miller J, ed. *Standards in fluorescence spectrometry*. London: Chapman & Hall, 49–67.
- Miranda V, Baker NR, Long SP.** 1981. Anatomical variation along the length of the *Zea mays* leaf in relation to photosynthesis. *New Phytologist* **88**, 595–605.
- Morales F, Cerovic ZG, Moya I.** 1996. Time-resolved blue-green fluorescence of sugar beet (*Beta vulgaris* L.) leaves: spectroscopic evidence for the presence of ferulic acid as the main fluorophore in the epidermis. *Biochimica et Biophysica Acta* **1273**, 251–262.
- Morales F, Cerovic ZG, Moya I.** 1998. Time-resolved blue-green fluorescence of sugar beet leaves. Temperature-induced changes and consequences for the potential use of blue-green fluorescence as a signature for remote sensing of plants. *Australian Journal of Plant Physiology* **25**, 325–334.
- Ounis A, Cerovic ZG, Briantais J-M, Moya I.** 2001. DE-FLIDAR: a new remote sensing instrument for the estimation of epidermal UV absorption in leaves and canopies. *EARSeL Proceedings* **1**, 196–204.
- Rasmussen DC, Dunford HB, Welinder KG.** 1995. Rate of enhancement of compound I formation of barley peroxidase by

- ferulic acid, caffeic acid, and coniferyl alcohol. *Biochemistry* **34**, 4022–4029.
- Riederer M, Schönherr J.** 1988. Development of plant cuticles: fine structure and cutin of *Clivia miniata* Reg. leaves. *Planta* **174**, 127–138.
- Schmidt HW, Schönherr J.** 1982. Development of plant cuticles: occurrence and role of non-ester bonds cutin of *Clivia miniata* Reg. leaves. *Planta* **156**, 380–384.
- Schnabl H, Weissenböck G, Scharf H.** 1986. *In vivo*-microspectrophotometric characterization of flavonol glucosides in *Vicia faba* guard and epidermal cells. *Journal of Experimental Botany* **37**, 61–72.
- Sharman BC.** 1942. Developmental anatomy of the shoot of *Zea mays* L. *Annals of Botany* **6**, 245–282.
- Stober F, Lichtenthaler HK.** 1993a. Characterization of the laser-induced blue, green and red fluorescence signatures of leaves of wheat and soybean grown under different irradiance. *Physiologia Plantarum* **88**, 696–704.
- Stober F, Lichtenthaler HK.** 1993b. Studies on the localization and spectral characteristics of the fluorescence emission of differently pigmented wheat leaves. *Botanica Acta* **106**, 365–370.
- Strack D, Keller H, Weissenböck G.** 1987. Enzymatic synthesis of hydroxycinnamic acid esters of sugar acids and hydroaromatic acids by protein preparations from rye (*Secale cereale*) primary leaves. *Journal of Plant Physiology* **131**, 61–73.
- Valeur B.** 1993. Fluorescent probes for evaluation of local physical and structural parameters. In: Schulman SG, eds. *Molecular luminescence spectroscopy methods and applications: Part 3*. New York: John Wiley & Sons, 25–84.
- Van Arendonk JJCM, Niemann GJ, Boon JJ, Lambers H.** 1997. Effects of nitrogen supply on the anatomy and chemical composition of leaves of four grass species belonging to the genus *Poa*, as determined by image-processing analysis and pyrolysis-mass spectrometry. *Plant, Cell and Environment* **20**, 881–897.
- Wiermann R.** 1981. Secondary plant products and cell and tissue differentiation. In: Stumpf PK, Conn EE, eds. *The biochemistry of plants*. London: Academic Press Inc. 85–116.